



# The Manufacture and Characterisation of Rosid Angiosperm-Derived Biochars Applied to Water Treatment

Gideon A. Idowu<sup>1,2</sup> · Ashleigh J. Fletcher<sup>1</sup>

© The Author(s) 2019

## Abstract

Marabu (*Dichrostachys cinerea*) from Cuba and aspen (*Populus tremula*) from Britain are two rosid angiosperms that grow easily, as a weed and as a phytoremediator, respectively. As part of scientific efforts to valorise these species, their barks and woods were pyrolysed at 350, 450, 550 and 650 °C, and the resulting biochars were characterised to determine the potential of the products for particular applications. Percentage carbon composition of the biochars generally increased with pyrolysis temperature, giving biochars with highest carbon contents at 650 °C. Biochars produced from the core marabu and aspen wood sections had higher carbon contents (up to 85%) and BET surface areas (up to 381 m<sup>2</sup> g<sup>-1</sup>) than those produced from the barks. The biochar porous structures were predominantly mesoporous, while micropores were developed in marabu biochars produced at 650 °C and aspen biochars produced above 550 °C. Chemical and thermal activation of marabu carbon greatly enhanced its adsorption capacity for metaldehyde, a molluscicide that has been detected frequently in UK natural waters above the recommended EU limit.

**Keywords** *Dichrostachys cinerea* · *Populus tremula* · Biochar · Characterisation · Water treatment

## Introduction

The rosids consist of 70,000 flowering plant species, which together constitute over one-fourth of all angiosperms. They comprise two large clades, eurosids I (Fabidae) and eurosids II (Malvidae), and their sister clade, the Vitaceae [49]. The rosids themselves belong to a super clade called the eudicot [23] and exhibit great diversity in ecology, behaviour and life forms, existing as trees, vines, herbs, shrubs, succulents and grasses. In addition, they contain biochemical mechanisms that permit them to exist in symbiotic and/or parasitic relationships with other organisms in the environment [39, 43]. While some rosids have economic importance as food crops (e.g.

*Manihot* spp. that forms part of staple foods for several millions of people in the tropical world) and edible fruits (e.g. *Carica* spp.), the vast majority of rosids are considered to be weeds, owing to their limited uses and applications. The two rosid species that are the focus of this study are *Dichrostachys cinerea* (a shrub from Cuba) and *Populus tremula* (a native British tree). These two angiosperms share taxonomic similarities within the Rosanae superorder, which is traditionally regarded as the clade for all rosids. The full taxonomic classifications of these angiosperms are shown in Table 1.

*Dichrostachys cinerea*, popularly known as marabu, is a woody shrub and weed considered a plague in Cuba, due to the invasive manner in which it grows. Originally from Africa, marabu was transplanted to Cuba for its attractive flowers. However, decline of the Cuban sugar industry left a vast area of arable land open to weeds, and Marabu spread unchecked, now covering over 1.7 million hectares of productive lands. The shrub is unsuitable for construction, does not float, and produces too much smoke to be useful for cooking or heating [38], and few scientific reports exist on the possible uses and applications of marabu. Abreu et al. [1] studied its pyrolysis and combustion processes and generated a kinetic model, describing its thermal decomposition characteristics. Another study by Gutiérrez et al. [15] considered heating marabu to augment energy mixes in order to improve electricity

**Electronic supplementary material** The online version of this article (<https://doi.org/10.1007/s12155-019-10074-x>) contains supplementary material, which is available to authorized users.

✉ Ashleigh J. Fletcher  
ashleigh.fletcher@strath.ac.uk

<sup>1</sup> Department of Chemical and Process Engineering, University of Strathclyde, James Weir Building, 75 Montrose Street, Glasgow G1 1XJ, UK

<sup>2</sup> Department of Chemistry, Federal University of Technology, PMB 704 Akure, Nigeria

**Table 1** Taxonomic classification of marabu and aspen, rosid precursors used in this study

Taxonomic hierarchy	Marabu ( <i>D. cinerea</i> )	Aspen ( <i>P. tremula</i> )
Kingdom	Plantae	Plantae
Subkingdom	Viridiplantae	Viridiplantae
Infrakingdom	Streptophyta	Streptophyta
Superdivision	Embryophyta	Embryophyta
Division	Tracheophyta	Tracheophyta
Subdivision	Spermatophytina	Spermatophytina
Class	Magnoliopsida	Magnoliopsida
Superorder	Rosanae	Rosanae
Order	Fabales	Malpighiales
Family	Fabaceae	Salicaceae
Genus	<i>Dichrostachys</i>	<i>Populus</i>
Species	<i>Dichrostachys cinerea</i>	<i>Populus tremula</i>

[43]; Integrated Taxonomic Information System, ITIS)

generation in the province of Cienfuegos in Cuba. Despite the shrub being the most abundant source of biomass in the province, the study concluded that the combustion of other biomasses, such as filter cake and energy cane, was more favourable, due to the longer payback period it would take to generate returns on the cost of investment in technologies for the harvesting of marabu. Additionally, an attempt was previously made to delignify marabu to assess the suitability of the cellulosic components for bioethanol production [44]. Notwithstanding these efforts, a yet unexplored application of marabu is the production of carbonaceous materials for possible treatment of water and other industrial liquids.

*Populus tremula*, called aspen in Britain, is a deciduous broad-leaf tree most commonly found in Scotland, where it currently occupies an estimated 160 hectares of woodland. The light weight of aspen wood makes it useful for making paddles, oars and surgical splints [33]. However, like marabu, scientific investigations into its other applications are limited. Scott and Piskorz [40] investigated the production of tar-like oil from aspen; Kalkreuth et al. [24] performed optical characterisation of aspen pyrolysis products using fluorescence and reflectance measurements. Both these works focused on the liquid products of aspen pyrolysis while the characteristics of aspen biochars have not been reported in literature.

Suitability of biochar for various potential applications depends on its characteristics, which in turn, depend, to a large extent, on the source biomass material pyrolysed [6, 17, 45]. In this study, marabu and aspen biochars were produced and characterised, with a view to optimising the carbons for various industrial applications, in particular, the removal of organic pollutants from water and other liquids. While there is some evidence that Cuba earns revenue from exporting cooking charcoal made from marabu wood [16], this study could help in identifying alternative uses for carbons derived from

marabu wood, for instance, in the Cuban rum industry, where millions of dollars are spent annually on carbon importation. Utilising marabu and aspen for biochar/carbon production would also offer some environmental benefits. Since pyrolysis, the method employed for the conversion of marabu and aspen biomasses in this study, takes place in the absence or limited supply of oxygen; the process could have advantage over alternate uses (e.g. combustion of marabu to produce charcoal) and over natural decomposition processes that release CO<sub>2</sub> to the atmosphere. Given that both aspen and marabu can be regularly coppiced, their conversion to biochar could allow for continual sequestration and storage of atmospheric CO<sub>2</sub> [50]. Moreover, the study could provide support for on-going efforts towards reviving aspen species in Britain.

## Materials and Methods

### Materials

Marabu (*D. cinerea*) wood was procured from the Caribbean nation of Cuba, while Aspen (*P. tremula*) wood was obtained from the Scottish Highlands. Marabu wood appears denser than aspen wood, based on observation of the dry stocks received in the laboratory. Four different sample types were derived from the two wood stocks. These were aspen wood, aspen bark, marabu wood and marabu bark. The ‘bark’ samples in both cases were taken from the peels obtained by scrapping the bark of the woods about 5 mm from the outermost part into the inner part. Aspen bark is dark brown, scaly and highly fibrous, while the core aspen wood is off-white in colour. Marabu bark is yellowish in colour, scaly, and non-fibrous. Marabu wood has a brown colour from the centre and up to a radius of about 1 cm from the centre, while the remaining part is yellowish in colour (Fig. 1).

The barks were separated from the core woods, and the different samples were divided into smaller pieces, ~ 5 mm



**Fig. 1** Marabu (L) and aspen (R) woods

in length, prior to pyrolysis. The pieces were washed with tap water and then with double distilled water to remove dust particles. Thereafter, they were dried in an oven at 105 °C for 24 h.

## Pyrolysis

Based on previous studies on wood pyrolysis, temperature is the main parameter influencing the characteristics of biochars, while holding time at the chosen pyrolysis temperature and inert gas flow rate have negligible effects [32, 42]. Thus, aspen and marabu precursors (2 g) were pyrolysed at 350, 450, 550 and 650 °C in this study. This temperature range is believed to result in biochars with desirable properties for various potential applications [34]. Pyrolysis was performed using a Carbolite Eurotherm 2132 assembly, consisting of a stainless-steel tubular reactor (220-mm long and 75-mm internal diameter), heated externally by an electric furnace. Argon (500 ml min<sup>-1</sup>) was continuously flowed over the sample at ambient temperature for the first 30 min to ensure any oxygen present in the tube at the beginning of the experiment was expunged; after which, the temperature was ramped (20 °C min<sup>-1</sup>) to the selected pyrolysis temperature, where it was held for 30 min. Once heating was complete, the furnace was cooled to 25 °C, with the argon flow maintained. The yield of biochar obtained for each precursor was calculated using Eq. 1.

$$\text{Biochar yield} = \frac{\text{weight of biochar produced (g)}}{\text{weight of precur sortaken (g)}} \cdot 100 \quad (1)$$

## Sample Coding System

The general naming system used for biochar samples obtained from the core woods is given by: first letter of the name of the wood, M or A and temperature of pyrolysis, e.g. 350. Biochars produced from the bark materials were given the suffix 'b' in addition to this general nomenclature. Thus, M350 refers to biochar sample from marabu wood pyrolysed at 350 °C; M350b is biochar sample obtained by pyrolysing marabu bark material at 350 °C. The unpyrolysed marabu and aspen woods were simply coded M and A respectively, while their corresponding unpyrolysed bark materials were named Mb and Ab, respectively.

## Analyses and Characterisation

### Fourier Transform Infrared Analysis

Surface functional groups of the biochars were determined by Fourier transform infrared (FTIR) (ABB IR Instrument MB 300 series). The FTIR analysis was performed using

Attenuated Total Reflectance (ATR), which made it possible to record IR spectra of the samples directly. Spectra of the powdered raw wood materials and those of the biochars produced were taken at 4 cm<sup>-1</sup> resolution between 600 and 4000 cm<sup>-1</sup> for a total of 32 scans. The measurements were taken in the transmittance mode and were recorded with the MB Horizon software. Assignment of surface functional groups to the IR bands observed was undertaken with reference to the works of Ozcimen and Ersoy-Mericboyu [31] and Figueiredo et al. [10].

### pH Determination

Determination of biochar pH is important to understanding their impact on the acid/base character of any system to which they are incorporated and to establish their suitability for specific purposes. The pH of each biochar was determined from a homogenised suspension of the char in water. A total of 20 ml of deionised water was added to 0.2 g of each biochar in a sample vial with lid. The mixture was intermittently shaken in the vial for 24 h, and pH measurements were performed using a calibrated Hanna pH metre.

### Elemental Carbon, Hydrogen and Nitrogen Analysis

Carbon, hydrogen and nitrogen (CHN) contents within the samples were determined via high temperature (1800 °C) oxidation to CO<sub>2</sub>, H<sub>2</sub>O and NO<sub>x</sub> (which were all reduced to N<sub>2</sub>), respectively. CHN analysis was performed using a Perkin Elmer 2400 CHN analyser. The samples were ground and homogenised before ~ 0.1 g of the sample to be analysed was loaded into the instrument. Oxygen content was determined using the same elemental analyser, operated in pyrolysis mode (without oxygen injection) at 1400 °C [13]. Analysis was performed on the raw marabu and aspen materials, as well as the biochars produced.

### Thermogravimetric Analysis

Proximate composition (i.e. moisture, volatile matter, fixed carbon and inorganic material) was determined for precursors and biochar samples using a NETZSCH STA 449F1 thermogravimetric analysis (TGA) instrument, programmed according to British standard BS 1016; ~ 20 mg of each sample was used. The sample was first held at 30 °C for 10 min under a flow of 50-ml min<sup>-1</sup> nitrogen gas. Still under nitrogen, the sample was heated to 127 °C at a rate of 20 °C min<sup>-1</sup> and held at this temperature for 10 min to remove moisture. The sample was subsequently heated to 927 °C and held at this temperature for 10 min to remove all volatile matter, before cooling to 827 °C at a rate of 50 °C min<sup>-1</sup>, where after the gas was switched to oxygen (50 ml min<sup>-1</sup>), held for 15 min to combust

all fixed carbon, leaving only inorganic matter. Data generated was processed using the associated software, STA 4491.

### Porous Structure Characterisation

Biochars were characterised for specific surface area, pore volume and pore size distribution using nitrogen adsorption at  $-196\text{ }^{\circ}\text{C}$  analysed using the Brunauer-Emmett-Teller (BET) model [19, 35]. BET analysis was performed using  $\sim 0.2\text{ g}$  of biochar and a Micrometrics ASAP 2420 system with nitrogen (99.99%) as adsorbate.

### Modification of Marabu Carbon

The marabu biochar pyrolysed at  $650\text{ }^{\circ}\text{C}$  (M650) was modified via a combination of chemical and thermal treatments in order to enhance its adsorption capabilities. A total of  $1.28\text{ g}$  of the biochar was refluxed in  $100\text{-ml}$   $7.5\text{-M}$   $\text{HNO}_3$  solution for  $48\text{ h}$ . This concentration has been shown to be suitable for the introduction of various oxygenated functional groups onto the surface of carbon materials [20, 21]. The refluxed marabu carbon was then washed thoroughly with distilled water to constant pH (6.58) and dried in an oven at  $105\text{ }^{\circ}\text{C}$ . This material was heated at  $400\text{ }^{\circ}\text{C}$  ( $20\text{ }^{\circ}\text{C min}^{-1}$ ) for  $8\text{ h}$  under a flow of argon gas ( $50\text{ ml min}^{-1}$ ) with the resulting ‘modified’ marabu carbon named M650m.

### Application of Marabu Carbons to Water Purification

Both M650m and its precursor, M650, were applied to the treatment of contaminated water, in particular, the removal of the organic pollutant metaldehyde. A total of  $0.2\text{ g}$  of the selected carbon was added to  $200\text{ ml}$  of water (at  $25\text{ }^{\circ}\text{C}$  and pH 6.8), pre-contaminated with metaldehyde ( $200\text{ mg L}^{-1}$ ). The vial containing each mixture was then placed in a shaker for continuous agitation. After a selected time interval ( $24$  or  $48\text{ h}$ ),  $5\text{ ml}$  of water was removed from each vial and filtered to remove fine particulates. The concentration of metaldehyde in each aliquot was determined using a gas chromatograph (Shimadzu 2014 model) equipped with flame ionisation detector (FID). Adsorption capacity of the carbons for metaldehyde was calculated in  $\text{mg g}^{-1}$  from Eq. 2.

Adsorption capacity

$$= \frac{(200-X)\text{ mg}}{\text{L}} \times 0.2\text{ L} \quad (2)$$

weight of carbon material (in g)

$X$  is the concentration of metaldehyde in water after  $24$  or  $48\text{ h}$ , respectively.

## Results and Discussion

### Yield of Biochars from Marabu and Aspen

Table 2 shows the percentage yield of biochar from marabu and aspen materials at various pyrolysis temperatures. The yield decreases with increasing pyrolysis temperature for the four different biomass materials (bark and core woods), with the highest yield obtained at  $350\text{ }^{\circ}\text{C}$  in all cases. This is not unexpected, as increasing pyrolysis temperature causes the removal of more volatile components, resulting in biochar products of reduced weight. However, the trend followed by the decrease in biochar yield with temperature appears to differ between the core wood and the bark materials for both marabu and aspen. While the decrease in biochar yield is gradual in the core aspen and marabu woods, there exists sharp decrease in biochar yield for the bark samples. This occurs between  $450$  and  $550\text{ }^{\circ}\text{C}$  for marabu bark (9.8% decrease) and between  $350$  and  $450\text{ }^{\circ}\text{C}$  for aspen (10.2% decrease). Such sharp decreases may be attributed to the influence of inorganic elements, which possibly catalyse the removal of more volatile organic constituents at temperatures in the interval where these decreases were observed. Wood barks are known to be generally higher in inorganic content than core wood, which contains more ordered layers of cellulose, hemicelluloses and lignin [5, 37]. More importantly, the results show that both marabu and aspen bark samples gave higher yields of biochar than the corresponding core woods at all pyrolysis temperatures. This difference in yield is more pronounced for aspen where the maximum yield obtained for the core wood was 27.7%, compared with 41.1% obtained from the bark at the same pyrolysis temperature ( $350\text{ }^{\circ}\text{C}$ ). This result is somewhat intriguing as aspen bark is very light and fibrous compared with the more solid aspen wood and would have been expected to be readily consumed by the high temperatures employed for pyrolysis.

**Table 2** Yield of biochars from aspen and marabu precursors at various pyrolysis temperatures

Sample	Biochar yield (%)	Sample	Biochar yield (%)
A350	$27.7 \pm 0.2$	M350	$43.1 \pm 0.8$
A450	$21.8 \pm 0.4$	M450	$36.6 \pm 0.3$
A550	$20.9 \pm 0.5$	M550	$31.7 \pm 0.9$
A650	$18.8 \pm 0.2$	M650	$29.6 \pm 0.8$
A350b	$41.1 \pm 0.6$	M350b	$48.0 \pm 0.3$
A450b	$30.9 \pm 0.3$	M450b	$43.7 \pm 0.6$
A550b	$29.1 \pm 1.2$	M550b	$33.9 \pm 0.3$
A650b	$26.9 \pm 0.7$	M650b	$32.3 \pm 0.4$

## pH and Surface Functionalities of Marabu and Aspen Biochars

Table 3 shows pH values recorded for biochars produced in this study; all materials were alkaline in nature, with the degree of alkalinity increasing with the temperature of pyrolysis. The result also shows that biochars produced from the bark of the woods have higher pH than those pyrolysed from the core woods, at all corresponding temperatures. The values generally range from 7.26 to 11.11 in biochars pyrolysed from the core marabu and aspen woods and from 8.92 to 11.92 in biochars pyrolysed from the barks. Baseline-corrected FTIR spectra of biochars obtained from the core woods and the barks (shown in Supporting Information, Figures S1–S4) reveal the effects of pyrolysis temperatures on surface functional group characteristics of marabu- and aspen-derived biochars. Peaks due to C–H stretching ( $3000\text{ cm}^{-1}$  to  $2600\text{ cm}^{-1}$ ) found in unpyrolysed samples decrease with increasing pyrolysis temperature and are completely lost for samples pyrolysed at  $650\text{ }^{\circ}\text{C}$  (i.e. M650 and A650). The decrease in features associated with C–H groups may be connected with the release of hydrogen molecules from the precursors during pyrolysis. Similarly, the broad O–H stretching peaks ( $3600\text{--}3200\text{ cm}^{-1}$ ) found in the precursors were lost in the biochar samples, while intense C–OH-stretching vibrations (at  $1000\text{ cm}^{-1}$ ) present in the precursors were also greatly reduced in the biochars. Loss of these features may be attributed to the removal of hydroxyl groups from cellulosic components in the precursors, leading to condensation of the original structures [26].

Apparently as a result of condensation, aromatic functional groups, which are not found in all the raw wood materials, are observed in the spectra of biochars produced at  $350\text{ }^{\circ}\text{C}$  and above, becoming more pronounced for the biochars produced at higher temperatures. Aromatic groups occur within the range  $930\text{--}702\text{ cm}^{-1}$  and may include mono- and di-substituted benzene derivatives. The bands provide evidence of cyclisation and the presence of aromatic groups on the surface of both aspen- and marabu-derived biochars. Peaks due to carboxyl-carbonates/carboxylic acid salt ( $1100\text{--}1600\text{ cm}^{-1}$ ) were also observed. While the FTIR analyses generally show no significant difference between the surface functional group compositions of biochars produced from the core wood of marabu and aspen, and those produced from their barks, it is notable that the peaks due to carbonates/carboxylic acid salt are more prominent in the spectra of biochars from the bark materials than in those from the core wood. This suggests that the bark precursors may have higher content of inorganic materials responsible for greater carboxylic salt formation in the biochars.

## Carbon, Hydrogen, Nitrogen and Oxygen Contents of Marabu and Aspen Biochars

Figure 2a shows the result of ultimate analyses performed to determine the CHNO contents of raw marabu and aspen precursors, as well as the resulting biochars produced at various pyrolysis temperatures. The results show that the carbon contents of the biochars are higher than the raw marabu and aspen precursors, even at low pyrolysis temperatures ( $350\text{ }^{\circ}\text{C}$ ), which increases as pyrolysis temperature is increased. For example, the carbon content of the raw marabu wood was 44.8%, increasing to 82.7% for the biochar produced at  $650\text{ }^{\circ}\text{C}$ ; similarly, for aspen, the raw wood had a carbon content of 43.9%, while the sample pyrolysed at  $650\text{ }^{\circ}\text{C}$  contained 85.6%. These results demonstrate the ability of the pyrolysis process to fix and concentrate carbon in biomass materials, and the maximum carbon contents obtained for marabu and aspen biochars are comparable to those reported for biochars from other tree species (e.g. 84.8% for apple tree biochar and 83.2% for oak tree biochar); higher than those reported for poplar wood (77.9%) and spruce wood (78.3%); and far higher than those reported for biochars from agricultural wastes such as corn stover (57.3%), rice husk (44.6%) and rice straw (49.9 %) ([22]; [25]; [30]). All biochars produced from the core woods have higher carbon contents than those produced from the bark materials at corresponding pyrolysis temperatures (Fig. 2b). The difference in carbon content is more pronounced in marabu-derived biochars than for aspen-derived materials, which may be attributed to the innate composition of the marabu bark precursor, influencing the removal of volatile materials during pyrolysis, and, consequently, dictating the composition of the various biochars produced. It is noteworthy that the marabu bark had a higher carbon content (46%) than the marabu wood (44.8%); however, this did not translate into higher carbon content for the bark-derived biochars, as the pyrolysis characteristics of this material caused retention of other non-carbonaceous substances, unlike the pyrolysis of the marabu core wood, which resulted in fixing more carbon in the resulting biochars.

As expected, the precursors have the highest content of hydrogen, notably highest in marabu (5.9% for the core wood and 6.2% for the bark). Hydrogen contents of the biochars decreased continuously with increasing pyrolysis temperature, indicating that more hydrogen species were evolved from the precursors as the pyrolysis temperature increased. Similarly, oxygen contents of all the biochars decreased with increasing pyrolysis temperature due to greater dehydration and deoxygenation. Unlike the carbon, hydrogen and oxygen contents, nitrogen content of the biochars appeared not to follow any particular trend over the range of temperatures employed for pyrolysis. This may be attributed to the lignocellulosic nature of the materials, having carbon, hydrogen and oxygen as the innate elements in their repeating polymeric structures [3],

**Table 3** pH, proximate compositions and textural properties of marabu and aspen precursors and their derived biochars

Sample	M	M350	M450	M550	M650	Mb	M350b	M450b	M550b	M650b	A	A350	A450	A550	A650	Ab	A350b	A450b	A550b	A650b
pH	-	7.76	8.89	9.21	11.11	-	9.01	10.62	11.66	11.92	-	7.26	8.64	8.75	9.63	-	8.92	9.92	9.71	10.43
%VM	73.1	37.3	25.7	16.1	11.8	72.6	45.5	39.5	27.4	24.0	72.4	34.9	28.3	18.0	15.0	72.0	43.6	26.1	22.8	20.8
%FM	20.3	58.9	63.1	73.9	78.1	17.4	36.8	42.5	53.9	54.0	22.0	53.9	61.6	76.1	79.5	21.8	46.4	60.9	68.6	71.9
%Ash	6.6	3.4	9.5	9.9	7.2	10.1	17.7	18.1	19.3	22.4	5.6	10.4	9.8	5.7	4.9	6.1	10.0	13.1	8.6	7.2
$v_{\mu}/\text{cm}^3 \text{g}^{-1}$	-	-	-	-	0.096	-	-	-	-	0.017	-	-	0.004	0.145	0.170	-	-	0.001	0.037	0.032
$S_{\text{BET}}/\text{m}^2 \text{g}^{-1}$	-	3	4	12	226	-	5	5	17	58	-	4	20	361	381	-	2	7	93	71
$\phi/\text{nm}$	-	13	5	10	1	-	33	40	8	11	-	14	37	-	2	-	35	16	26	27

VM, volatile matter; FM, fixed matter;  $v_{\mu}$ , micropore volume; SBET, surface area determined using BET method;  $\phi$ , average pore width

whereas nitrogen is only taken up from the soil via the activities of nitrogen-fixing bacteria. The nitrogen contents of the materials may, therefore, vary widely, depending on environmental factors and the particular part of the shrub obtained for pyrolysis. Consequently, the nitrogen content of the biochars may not be expected to show a consistent trend compared with carbon and hydrogen, which are intrinsic structural components of the precursors.

### Proximate Compositions of Marabu and Aspen Biochars

The dry weight proximate compositions (volatile matter, fixed matter and residual ash) of the biochars were obtained from thermogravimetric analysis and are presented in Table 3. The results show that the volatile matter contents of the biochars decreased as pyrolysis temperature increased. This is expected, since pyrolysis at higher temperatures causes more volatile components to be driven off, thereby producing biochars with lower amounts of volatile matter. This trend is the same for biochars produced from the core wood and bark of both marabu and aspen and is consistent with the results obtained for the hydrogen content of the biochars. Fixed-matter contents increased with pyrolysis temperature, both for biochars from the core woods and their barks. The percentage-fixed matter is generally higher in biochars from core woods than in biochars produced from the corresponding barks, at all temperatures studied, although the range of values obtained is narrower for aspen than for marabu. Fixed-matter content is a measure of the carbon content of biochars, otherwise called fixed carbon [27, 36]. Results obtained for the percentage fixed-matter contents are, therefore, consistent with the carbon content of the biochars determined from elemental (CHN) analyses for both marabu and aspen precursors.

Ash content of the biochars did not vary uniformly with pyrolysis temperature; however, biochars produced from the bark materials have higher ash contents than biochars produced from core woods at the same temperatures, likely related to the higher inorganic content of the barks compared with the core woods. The result is in agreement with the FTIR analyses (discussed in the 'pH and Surface Functionalities of Marabu and Aspen Biochars' section), which showed more pronounced carbonates/carboxylic acid salt peaks for the bark biochars. Carbonate, in the form of CaO residue, is generally associated with the ash contents of woods [29]. The result is also consistent with the higher pH values (greater alkalinity) of the bark biochars compared with the biochars produced from the core woods. Despite the higher yields of biochars from both marabu and aspen barks, the low carbon contents and high ash contents of these biochars imply that they are of lower quality compared with those from the core woods. These higher yields may be due to contributions from

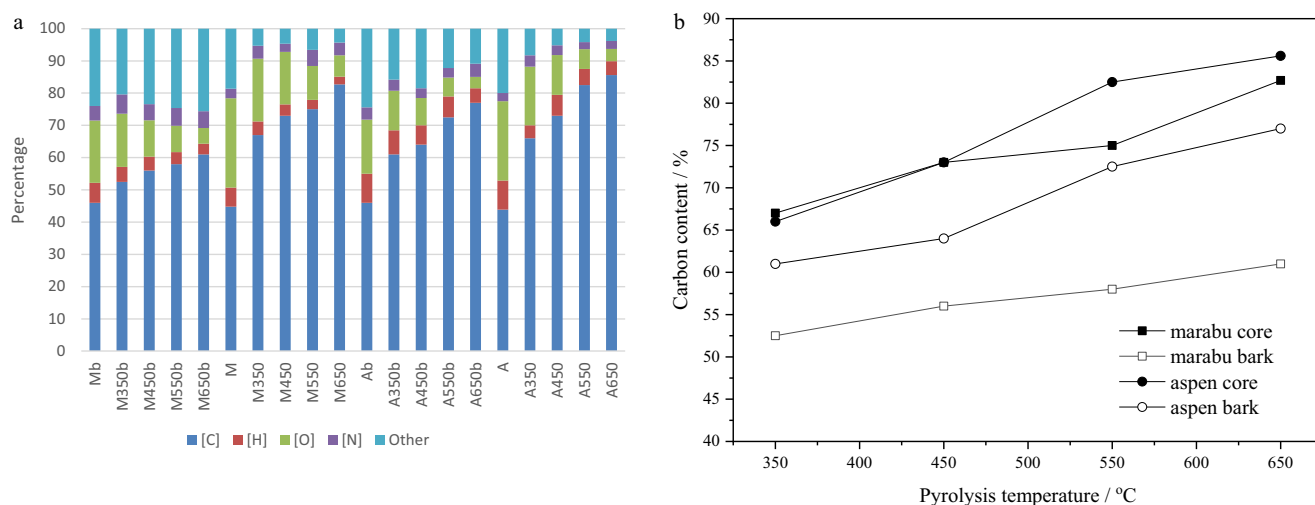


**Fig. 2** **a** Carbon, hydrogen, nitrogen and oxygen (CHNO) contents of marabu and aspen precursors and their derived biochars. **b** Comparison of carbon contents of biochars from marabu and aspen core woods and barks

inorganic substances present in the bark materials and not the more desirable fixed organic carbon content.

### Porous Structure Characteristics of Marabu and Aspen Biochars

Isotherms for nitrogen sorption at  $-196\text{ }^{\circ}\text{C}$  were obtained for all biochars produced in this study, and analysis provided textural data presented in Table 3. Isotherms obtained for marabu-derived biochars show Type II/IVa character according to the recognised isotherm classification [7, 19, 47]. It is not possible to attribute a single isotherm type to the shapes obtained for the nitrogen sorption characteristics of the biochars. This is due to the lack of a plateau at higher relative pressures in the isotherms, as well as the observation of hysteresis loops in all cases. The isotherms show small uptake in the low relative pressure region, with a gradual increase in uptake with increasing pressure before a final upward curve for uptake, indicative of condensation in mesopores. Such isotherm shapes are indicative of mesoporous or non-porous systems and explains why the quantity of nitrogen adsorbed and surface areas obtained are low in comparison with other carbonaceous sorbents. M650 shows the greatest adsorption potential with a higher uptake in the micropore region, in addition to extended mesoporous structure and capillary condensation therein [12, 19, 41].

Similar to M650, there is evidence of microporous structures in aspen biochars, particularly A550 and A650, which both exhibit enhanced uptakes at low relative pressure. All aspen-derived chars again show capillary condensation effects at higher pressures, indicating mesoporous character as well, and Type II/IVa [47] isotherms as a result. The development of micropores in the aspen samples and M650 is also evident in their pore size distributions (see Supporting Information, Figures S7–S10). Micropore volumes, determined using  $t$  plot

analysis, and shown in Table 3, confirm the development of micropore character in these materials, however, the volumes obtained are modest compared with predominantly microporous sorbents (up to  $0.170\text{ cm}^3\text{ g}^{-1}$ ). The micropores developed in these samples do offer enhanced adsorbate–adsorbent interactions and adsorption energy due to their smaller size and closer proximity of their adsorption surfaces [19]. Biochars produced from the bark materials exhibit Type II/IVa [47] isotherms for all pyrolysis temperatures in the case of both woods (see Supporting Information, Figures S5–S6), again indicating mesoporous character, which dominates for marabu and is developed in tandem with microporosity for aspen. In general, nitrogen sorption showed a higher level of uptake for the core woods than for the barks; in addition to their comparative lack of microporous structure, the bark biochars have low carbon and high ash contents, which may also contribute to their poor adsorption capabilities. Isotherm hysteresis is often associated with mesoporous structures [48], and the hysteresis found in the biochars is similar to that described as Type H4, with the branches being nearly horizontal and parallel to each other over a wide relative pressure range. Type H4 hysteresis is said to be associated with narrow slit-like pores in adsorbent materials [2]; in each case presented here, hysteresis continued to the lowest attainable pressures (i.e. the two branches did not converge even at low pressures), an unusual feature believed to be due to the irreversible uptake of molecules in pores of comparable width as the adsorbate molecules [19].

Table 3 shows the variation of average pore size (width) and BET surface area with pyrolysis temperature for marabu and aspen biochars. The pore width data confirm the formation of microporous structures in aspen biochars and M650. Average pore size plots of all the bark biochars show that the pore widths are far higher than for the wood biochars, consistent with their largely mesoporous structures, as revealed by

the isotherms obtained for these samples. BET surface area increased for samples created using pyrolysis temperatures up to 550 °C for all precursors. For biochars produced from marabu, both wood and bark, the surface area increased further and more significantly at 650 °C (increasing from 12 m<sup>2</sup> g<sup>-1</sup> at M550 to 226 m<sup>2</sup> g<sup>-1</sup> for M650). For aspen precursors, however, the surface area increase was more modest, as extensive surface area was developed at the lower temperatures (361 m<sup>2</sup> g<sup>-1</sup> at A550 to 381 m<sup>2</sup> g<sup>-1</sup> for A650), as shown in Table 3. The surface area of carbonaceous materials is composed predominantly of the internal surface area, while the external surface contributes little to the total value [11, 28]. The increase in surface area at higher temperatures observed here suggests the creation of more open porosity. The reduction of surface area seen for A650b may be due to a loss of porosity, resulting from blockage of pores by materials eliminated at the high temperature in that particular precursor [34]. In general, biochars from the core aspen and marabu woods all exhibited greater BET surface area than the biochars obtained from the barks. The maximum BET surface areas obtained here are below those reported for apple tree biochar (545 m<sup>2</sup> g<sup>-1</sup>) and oak tree biochar (398 m<sup>2</sup> g<sup>-1</sup>) [22]. They are, however, much higher than those reported for biochars from poplar wood (55 m<sup>2</sup> g<sup>-1</sup>) and spruce wood (40 m<sup>2</sup> g<sup>-1</sup>) [25], as well as biochars from agricultural residues, such as apricot stone (11 m<sup>2</sup> g<sup>-1</sup>), hazelnut shell (15 m<sup>2</sup> g<sup>-1</sup>), grape seed (14 m<sup>2</sup> g<sup>-1</sup>), chestnut shell (< 1 m<sup>2</sup> g<sup>-1</sup>) and switch grass (1 m<sup>2</sup> g<sup>-1</sup>) [18, 31]. Of all biochars produced from the core wood materials, aspen biochars demonstrated higher surface areas than marabu biochars produced at corresponding temperatures, suggesting that they may have greater potential as adsorbents than marabu biochars.

### Metaldehyde Removal from Water by Marabu Carbon

Creation of porous character offers the use of carbonaceous sorbents in a range of applications. Here, the biochars produced were tested for removal capacity of a persistent organic pollutant. Sample M650 was selected as it offered a combination of relevant pore width and relatively high surface area, as required in such aqueous phase adsorption applications. Metaldehyde is a toxic organic compound used in pesticide formulations to prevent attack of slugs and snails on crops. The high solubility and mobility of metaldehyde in water have caused it to be found in surface waters at levels above the European and UK standard limit of 0.1 µg L<sup>-1</sup> for individual pesticides in drinking water [4, 8]. Metaldehyde is not easily removed from water by conventional treatment processes and thus poses a challenge to water companies who abstract raw water from rivers and reservoirs to produce drinking water [9]. As part of an initial effort towards finding applications for marabu biochars in this study, batch adsorption experiments for metaldehyde removal from water were performed. Water

contaminated with metaldehyde (200 mg L<sup>-1</sup>) was treated with the biochar sample M650 and its modified form, M650m, allowing a comparison of oxygen-containing moieties for remediation of this species. Gas chromatography–mass spectrometry (GC-MS) analyses of the water samples following sorption contact times of 24 and 48 h revealed that the concentration of metaldehyde was drastically reduced in the water sample treated with the modified marabu biochar (M650m), as against the water sample treated directly with M650 for both treatment times, as shown in Table 4 (see also Supporting Information, Figures S11–S14). Based on the residual concentration of metaldehyde in the water samples after 48 h, adsorption capacities of M650 and M650m for metaldehyde were determined to be 26.6 mg g<sup>-1</sup> and 168.1 mg g<sup>-1</sup>, respectively. This large difference between the adsorption capacities of M650 and M650m shows, in the first instance, that a carbon material with enhanced adsorption capacity was successfully generated from marabu biochar, M650. More importantly, the results show that the modified marabu carbon (M650m) is effective for the removal of metaldehyde from water and offers a potential route towards material development in this area.

Examination of the porous structure characteristics of M650m revealed that it was non-porous, which contrasts markedly with the data obtained for the original material, M650, which had a surface area of 226 m<sup>2</sup> g<sup>-1</sup>. This reduction in accessible area may be due to functionalisation of the surface, causing alterations in the porous structure and restricting gas molecules entering the pores [51]. Thus, the increased adsorption capacity of M650m may not be attributable to any improvement in the porous structure characteristics of the material. Conversely, there may be influence from the changes in the external surface character, and FTIR analyses of M650m and M650 (see Supporting Information, Figure S15) reveal the presence of oxygenated functional groups on the surface of M650m that are not present for M650. These functionalities most likely result from the oxidation of the aromatic groups present in the biochar M650 and are mainly comprised of carboxylic acid groups, indicated by bands at 1200 cm<sup>-1</sup> and 1700 cm<sup>-1</sup> and quinines, indicated by a band at 1600 cm<sup>-1</sup>. It may therefore be inferred that the newly introduced surface functionalities are responsible for the higher adsorption capacity of the material M650m, as they may enhance adsorption of metaldehyde. In particular, the oxygen-containing carboxylic acid functionalities present on the surface of M650m offer potential hydrogen bonding interactions (via –O: and –OH) with available hydrogen and oxygen sites on metaldehyde. This is consistent with previous studies, which have shown that metaldehyde molecules associate by hydrogen bonding and may indeed be adsorbed from aqueous solution by this mechanism [14, 46]. The high adsorption capacity of M650m for metaldehyde means that marabu carbons, if properly engineered, have significant

**Table 4** Concentration of metaldehyde (mg L<sup>-1</sup>) in water samples treated with marabu carbons

Sample	After 24 h	After 48 h
M650	183.1	171.1
M650m	38.5	15.7

potential for the removal of organic pollutants from water and wastewaters.

## Conclusions

Biochars produced from barks and core woods of marabu and aspen were characterised, showing that core woods have higher carbon contents and surface areas than those obtained from pyrolysis of barks, particularly at higher temperatures. Micropores were developed in several samples, notably marabu biochars obtained at 650 °C and aspen biochars produced from 550 °C, suggesting that the woods offer different initial structures that react differently to thermal treatment, producing a range of final materials. Oxidation of marabu biochar enhanced its adsorption capacity for the molluscicide metaldehyde from water, indicating the potential of biochar materials for utilisation to remove organic pollutants from wastewaters.

**Funding Information** GAI received financial support from the University of Strathclyde and the British Government via Commonwealth Scholarships.

**Open Access** This article is distributed under the terms of the Creative Commons Attribution 4.0 International License (<http://creativecommons.org/licenses/by/4.0/>), which permits unrestricted use, distribution, and reproduction in any medium, provided you give appropriate credit to the original author(s) and the source, provide a link to the Creative Commons license, and indicate if changes were made.

## References

- Abreu R, Conesa J, Foppa E, Romero O (2012) Kinetic analysis: simultaneous modelling of pyrolysis and combustion processes of *Dichrostachys cinerea*. *Biomass Bioenergy* 36:170–175
- Adelkhani H, Ghaemi M, Ruzbehani M (2011) Evaluation of the porosity and the nano-structure morphology of MnO<sub>2</sub> prepared by pulse current electrodeposition. *Int J Electrochem Sci* 6:123–135
- Ahmad M, Rajapaksha AU, Lim JE, Zhang M, Bolan N, Mohan D, Vithanage M, Lee SS, Ok YS (2014) Biochar as a sorbent for contaminant management in soil and water: a review. *Chemosphere* 99:19–33
- Asfawa A, Maher K, Shucksmith JD (2018) Modelling of metaldehyde concentrations in surface waters: a travel time based approach. *J Hydrol* 562:397–410
- Basu P (2013) *Biomass gasification, pyrolysis and torrefaction: practical design and theory*, second edn. Elsevier Inc.
- Blackwell P, Riethmuller G, Collins M (2009) Biochar application to soil. In: Lehmann J, Joseph S (eds) *Biochar for environmental management*. Earthscan, London
- Brunauer S, Deming LS, Deming WE, Teller E (1940) On a theory of the van der Waals adsorption of gases. *J Am Chem Soc* 62:1723–1732
- Castle GD, Mills GA, Gravell A, Jones L, Townsend I, Cameron DG, Fones GR (2017) Review of the molluscicide metaldehyde in the environment. *Environ Sci Water Res Technol* 3:415–428
- Castle GD, Mills GA, Bakir A, Gravell A, Schumacher M, Snow K, Fones GR (2018) Measuring metaldehyde in surface waters in the UK using two monitoring approaches. *Environ. Sci Process Impacts* 20:1180–1190
- Figueiredo JL, Pereira MFR, Freitas MMA, O'rao JJM (1999) Modification of the surface chemistry of activated carbons. *Carbon* 37:1379–1389
- Fletcher A, Yuzak Y, Thomas K (2006) Adsorption and desorption kinetics for hydrophilic and hydrophobic vapors on activated carbon. *Carbon* 44(5):989–1004
- Fletcher AJ, Kennedy MJ, Zhao XB, Bell JG, Thomas KM (2008) Adsorption of organic vapour pollutants on activated carbon. In: Mota JP, Lyubchik S (eds) *Recent advances in adsorption processes for environmental protection and security*. Springer, pp 29–54
- Gehre M, Strauch G (2003) High-temperature elemental analysis and pyrolysis techniques for stable isotope analysis. *Rapid Commun Mass Spectrom* 17(13):1497–1503. <https://doi.org/10.1002/rcm.1076>
- Gupta V, Gupta B, Rastogi A, Agarwal S, Nayak A (2011) A comparative investigation on adsorption performances of mesoporous activated carbon prepared from waste rubber tire and activated carbon for a hazardous azo dye – Acid Blue 113. *J Hazard Mater* 186: 891–901
- Gutierrez AS, Cabello Eras JJ, Hens L, Vande Castele C (2016) The biomass based electricity generation potential of the province of Cienfuegos, Cuba. *Waste Biomass Valor* 8:2075–2085. <https://doi.org/10.1007/s12649-016-9687-x>
- Havana (2015) Cuba exports millions in marabou coal. Available at <https://havanatimes.org/?p=109126> (Accessed 23/01/2019)
- Hossain MK, Strezov V, Yin Chan K, Ziolkowski A, Nelson PF (2011) Influence of pyrolysis temperature on production and nutrient properties of wastewater sludge biochar. *J Environ Manag* 92: 223–228
- Imam T, Capareda S (2012) Characterisation of bio-oil, syn-gas and bio-char from switch grass pyrolysis at various temperatures. *J Anal Appl Pyrolysis* 93:170–177
- IUPAC (1982) Reporting physisorption data for gas/solid systems, with special reference to the determination of surface area and porosity. *Pure Appl Chem* 54(11):2201–2218
- Jia YF, Thomas KM (2000) Adsorption of cadmium ions on oxygen surface sites in activated carbon. *Langmuir* 16:1114–1122
- Jia YF, Xiao B, Thomas KM (2002) Adsorption of metal ions on nitrogen surface functional groups in activated carbons. *Langmuir* 18:470–478
- Jindo K, Mizumoto H, Sawada Y, Sanchez-Monedero MA, Sonoki T (2014) Physical and chemical characterization of biochars derived from different agricultural residues. *Biogeosciences* 11: 6613–6621. <https://doi.org/10.5194/bg-11-6613-2014>
- Judd WS, Olmstead RG (2004) A survey of tricolpate (eudicot) phylogeny. *Amer J Bot* 91:1627–1644
- Kalkreuth W, Brouillard D, Roy C (1986) Optical and chemical characterisation of solid residues obtained from vacuum pyrolysis of wood (Aspen poplar). *Biomass* 10(1):27–45
- Kloss S, Zehetner F, Dellantonio A, Hamid R, Ottner F, Liedtke V, Schwanninger M, Gerzabek MH, Soja G (2012) Characterization of slow pyrolysis biochars: effects of feedstocks and pyrolysis

- temperature on biochar properties. *Journal of environmental quality* 41(4):990-1000.
26. Lee JW, Kidder M, Evans BR, Paik S, Buchanan AC, Garten CT, Brown RC (2010) Characterization of biochars produced from corn stovers for soil amendment. *Environ Sci Technol* 44:7970–7974
  27. Leng L, Huang H, Li H, Li J, Zhou W (2019) Biochar stability assessment methods: a review. *Sci Total Environ* 647:210–222
  28. Manocha SM (2003) Porous carbon. *Sadhana* 28:335–348
  29. Mohan D, Rajput S, Singh VK, Steele PH, Pittman CU Jr (2011) Modelling and evaluation of chromium remediation from water using low cost bio-char, a green adsorbent. *J Hazard Mater* 188:319–333
  30. Mullen CA, Boateng AA, Goldberg NM, Lima IS, Laird DA, Hicks KB (2010) Bio-oil and bio-char production from corn cobs and stover by pyrolysis. *Biomass Bioenergy* 34:67–74
  31. Özçimen D, Ersoy-Meriçboyu A (2010) Characterization of bio-char and bio-oil samples obtained from carbonization of various biomass materials. *Renew Energy* 35:1319–1324
  32. Ozcimen D, Karaosmanoglu F (2004) Production and characterization of bio-oil and biochar from rapeseed cake. *Renew Energy* 29:779–787
  33. Parrott J (2009) *Aspen in Scotland: biodiversity and management*. Available at <https://digitalcommons.usu.edu> (Accessed 21/01/2019)
  34. Pastor-Villegas JC, Dura'n-Valle J, Valenzuela-Calahorra C, Go'mez-Serrano V (1998) Organic chemical structure and structural shrinkage of chars prepared from rockrose. *Carbon* 36(9):1251–1256
  35. Reichenauer G, Scherer GW (2000) Nitrogen adsorption in compliant materials. *J Non-Cryst Solids* 277:162–177
  36. Ronsse F, Van Hecke S, Dickinson D, Prins W (2013) Production and characterization of slow pyrolysis biochar: influence of feedstock type and pyrolysis conditions. *GCB Bioenergy* 5(2):104–115
  37. Rowell RM (ed) (2012) *Handbook of wood chemistry and wood composites*, Second edn. CRC Press, Boca Raton
  38. Ruiz Sinoga JD, Remond Noa R, Fernandez Perez D (2010) An analysis of the spatial colonization of scrubland intrusive species in the Itabo and Guanabo watershed, Cuba. *Remote Sens* 2(3):740–757. <https://doi.org/10.3390/rs2030740>
  39. Schonenberger J, Von Balthazar M (2006) Reproductive structures and phylogenetic framework of the rosids-progress and prospects. *Plant Syst Evol* 260:87–106
  40. Scott DS, Piskorz J (1982) The flash pyrolysis of aspen-poplar wood. *Can J Chem Eng* 60(5):666–674
  41. Sing KSW, Everett DH, Haul RAW, Moscou L, Pierotti RA, Rouquerol J, Siemieniowska T (1985) Reporting physisorption data for gas/solid systems. *Pure Appl Chem* 57(4):603–619
  42. Smith M (2011) Effect of pyrolysis conditions on willow biochar characteristics. Master's dissertation in chemical and process engineering, University of Strathclyde, Glasgow
  43. Soltis DE, Soltis PS, Endress PK, Chase MW (2005) Phylogeny and evolution of Angiosperms. Sinauer, Sunderland
  44. Soudham VP (2009) Acetosolv delignification of *Dichrostachys cinerea* biomass for ethanol production. Master thesis. University College of Borås, Sweden
  45. Steinbeiss S, Gleixner G, Antonietti M (2009) Effect of biochar amendment on soil carbon balance and soil microbial activity. *Soil Biol Biochem* 41:1301–1310
  46. Tao B, Fletcher AJ (2013) Metaldehyde removal from aqueous solution by adsorption and ion exchange mechanisms onto activated carbon and polymeric sorbents. *J Hazard Mater* 244 – 245:240–250
  47. Thommes M, Kaneko K, Neimark AV, Olivier JP, Rodriguez-Reinoso F, Rouquerol J, Sing KS (2015) Physisorption of gases, with special reference to the evaluation of surface area and pore size distribution (IUPAC Technical Report). *Pure Appl Chem* 87(9-10):1051–1069
  48. Von V (2009) Hysteresis phenomena in mesoporous materials. PhD thesis. Universität Leipzig, Germany
  49. Wang H, Moore MJ, Soltis PS, Bell CD, Brockington SF, Alexandre R, Davis CC, Latvis M, Manchester SR, Soltis DE (2009) Rosid radiation and the rapid rise of angiosperm-dominated forests. *Proc Natl Acad Sci USA* 106(10):3853–3858
  50. Woolf D, Amonette JE, Street-Perrott FA, Lehmann J, Joseph S (2010) Sustainable biochar to mitigate global climate change. *Nat Commun* 1:1–9
  51. Yang X, Zhang S, Ju M, Liu L (2019) Preparation and modification of biochar materials and their application in soil remediation. *Appl Sci* 9:1365–1389. <https://doi.org/10.3390/app9071365>

**Publisher's Note** Springer Nature remains neutral with regard to jurisdictional claims in published maps and institutional affiliations.